Final Report: DOE Award No. DE-SC0014058
FUNDAMENTAL STUDIES OF BIFUNCTIONAL CATALYSTS FOR TANDEM REACTIONS

Department of Chemical and Biological Engineering
University of Wisconsin – Madison
Principal Investigator: James A. Dumesic

Grant period: August 1, 2015 – 2022

Abstract

During the past few years of our funding from DOE Basic Energy Sciences, we have focused on the catalytic conversion of biomass-derived 5-hydroxymethyl furfural (HMF) as a platform molecule for sustainable synthesis of value-added chemicals. The combination of the diene and aldehyde functionalities in HMF enables catalytic production of acetalized HMF derivatives with diol or epoxy reactants to allow reversible synthesis of norcantharimide derivatives upon Diels-Alder reaction with maleimides. Whereas the electron-withdrawing nature of aldehyde group inhibits the reactivity of diene group in HMF to undergo Diels-Alder reactions with dienophiles, by converting the aldehyde group in HMF to an electron-donating hydroxyl group, HMF can append maleimide-based chemicals through Diels-Alder coupling. Acetalization of HMF not only produces an electron-rich diene for Diels-Alder reaction, but it also alters the reversibility of acetal formation and thereby allows for the controlled release of chemicals by hydrolysis. Therefore, we synthesized various norcantharimide derivatives from biomass-derived HMF by acetalization over an acid catalyst, Amberlyst-15, followed by Diels-Alder reaction with maleimide. The norcantharimides release the starting materials by retro Diels-Alder reaction that is triggered by acetal hydrolysis under acidic (≤pH 3) conditions.

In subsequent work, we explored the synthesis and properties of functional polyurethanes and polyesters with tunable properties from biomass-derived (HMF)-Acetone-HMF (HAH) monomers. HAH can be selectively hydrogenated over Cu and Ru catalysts to produce partially-hydrogenated HAH (PHAH) and fully-hydrogenated HAH (FHAH). HAH contains functional groups, including hydroxyl, furan, enone, and ketone functionalities, that can be exploited to further tune the polymer properties. The π-electron conjugation between the enone and furan groups in HAH monomer stabilizes the furan group to prevent the uncontrolled degradation of furans during reactions, such as etherification. Therefore, HAH is a renewable monomer that can be used to synthesize polymers, having high molecular weight, symmetric functionalities, an inexpensive production price, and being derived from renewable resources without competition with food resources. We demonstrated the synthesis of functional polyurethanes and a renewable polyester from HAH-derived monomers, and 4,4'-methylenebis(phenyl isocyanate) (MDI).

We showed that it is essential to be able to selective hydrogenate C=C double bonds in HAH to be able to achieve effective Diels Alder reactions of the furan ring. Therefore, we studied the hydrogenation at temperatures from 313 – 393 K of HAH over Pd, Ru, and Cu based catalysts. HAH was selectively hydrogenated to produce partially-hydrogenated monomers (PHAH) over Cu and Ru catalysts and to fully-hydrogenated HAH monomers (FHAH) over the Ru catalyst. Pd based catalysts yielded a mixture of partially and fully hydrogenated monomers. Reaction kinetics models were employed to quantify the kinetic behavior for hydrogenation over Ru, Cu, and Pd catalysts. A 5-step pathway exhibited over Pd and Ru catalysts consists of both series and parallel reaction steps, where HAH is both converted to fully hydrogenated products

sequentially via series reactions of partially hydrogenated intermediates, as well as converted directly in parallel reactions to form the fully hydrogenated products. In contrast, a 3-step pathway over the Cu catalyst consists only of the consecutive reaction steps, where the final product was formed via series reactions of intermediate products. Additionally, reaction over the Cu catalyst did not hydrogenate the furan rings of the HAH molecule and yielded a different final product than those hydrogenation over Pd and Ru catalysts. Using the results from our detailed reaction kinetics studies, we developed universal conditions for the maximum production of the various hydrogenated products for both batch and plug flow systems.

In subsequent work, we employed reaction schemes to optimize the yields of products from selective hydrogenations of HAH in isopropanol solvent and in the presence of liquid water. Reaction schemes consisting of 7, 9, and 11 steps were examined to describe the rates of formation of the observed products and reaction intermediates for hydrogenation of HAH over Ru and Pd catalysts, and a 3-step scheme was studied over Cu catalysts. Rate constants and activation energies were calculated using these reaction schemes, and we then apply these reaction schemes to explore the effects of water addition on the hydrogenation pathways. The effects of water addition to isopropanol (IPA) solvents on the hydrogenation of HAH were markedly different over Pd, Ru, and Cu catalysts. Over the Pd catalyst, the addition of water to IPA increased hydrogenation rates and promoted hydrogenation of furan rings. The addition of water to IPA yielded significant carbon losses over the Ru catalyst, and slowed hydrogenation steps over Cu, while significantly inhibiting hydrogenation of the ketone group. This behavior opened routes toward increased production rates of PHAH=O (a partially hydrogenated form of HAH containing a C=O bond), a product in which the diene groups of the furan rings were not hydrogenated. Addition of water also allowed increased feed concentrations of HAH that were previously not possible in pure IPA solvents.

Final Report

During the past few years of our funding from Basic energy Sciences, we have focused on the catalytic conversion of biomass-derived 5-hydroxymethyl furfural (HMF) as a platform molecule for sustainable synthesis of value-added chemicals. We have reported catalytic strategies to synthesize and release chemicals for applications in fine chemicals, such as drugs and polymers from HMF. The combination of the diene and aldehyde functionalities in HMF enables catalytic production of acetalized HMF derivatives with diol or epoxy reactants to allow reversible synthesis of norcantharimide derivatives upon Diels-Alder reaction with maleimides. Reverse-conversion of the acetal group to an aldehyde yields mismatches of the molecular orbitals in norcantharimides to trigger retro Diels-Alder reaction at ambient temperatures and releases reactants from the coupled molecules under acidic conditions. These strategies provide for the facile synthesis and controlled release of high-value chemicals.

Synthesis and release of chemicals, which are of critical importance for fine chemicals, involve the following key chemical challenges: (i) designing a material that provides chemical bonding sites, (ii) incorporating a mechanism that releases the chemical at ambient temperatures, and (iii) controlling the release mechanism at the desired target. We showed that these challenges can be fulfilled by the synthesis of materials containing a furan group conjugated to an aldehyde group, such as in HMF. A key chemical property of HMF that has not been utilized previously is this conjugation between the diene and aldehyde functionalities. In particular, the electron-withdrawing nature of aldehyde group inhibits the reactivity of diene group in HMF to undergo

Diels-Alder reactions with dienophiles. However, by converting the aldehyde group in HMF to an electron-donating hydroxyl group, HMF can append maleimide-based chemicals through Diels-Alder coupling. Moreover, acetalization of HMF not only produces an electron-rich diene for Diels-Alder reaction, but it also alters the reversibility of acetal formation and thereby allows for the controlled release of chemicals by hydrolysis. Accordingly, the combination of acetalized HMF and maleimide provides a catalysis platform to control the synthesis and release of chemicals. Therefore, we synthesized various norcantharimide derivatives from biomass-derived HMF by acetalization over an acid catalyst, Amberlyst-15, followed by Diels-Alder reaction with maleimide. The norcantharimides release the starting materials by retro Diels-Alder reaction that is triggered by acetal hydrolysis under acidic (≤ pH 3) conditions. The synergy of the furan and aldehyde functionalities in HMF thus enables the production of therapeutic and polymeric materials, and the controlled chemical release at ambient temperatures (35-60ºC). Figure 1 describes reaction schemes for the synthesis and release of norcantharimide derivatives.

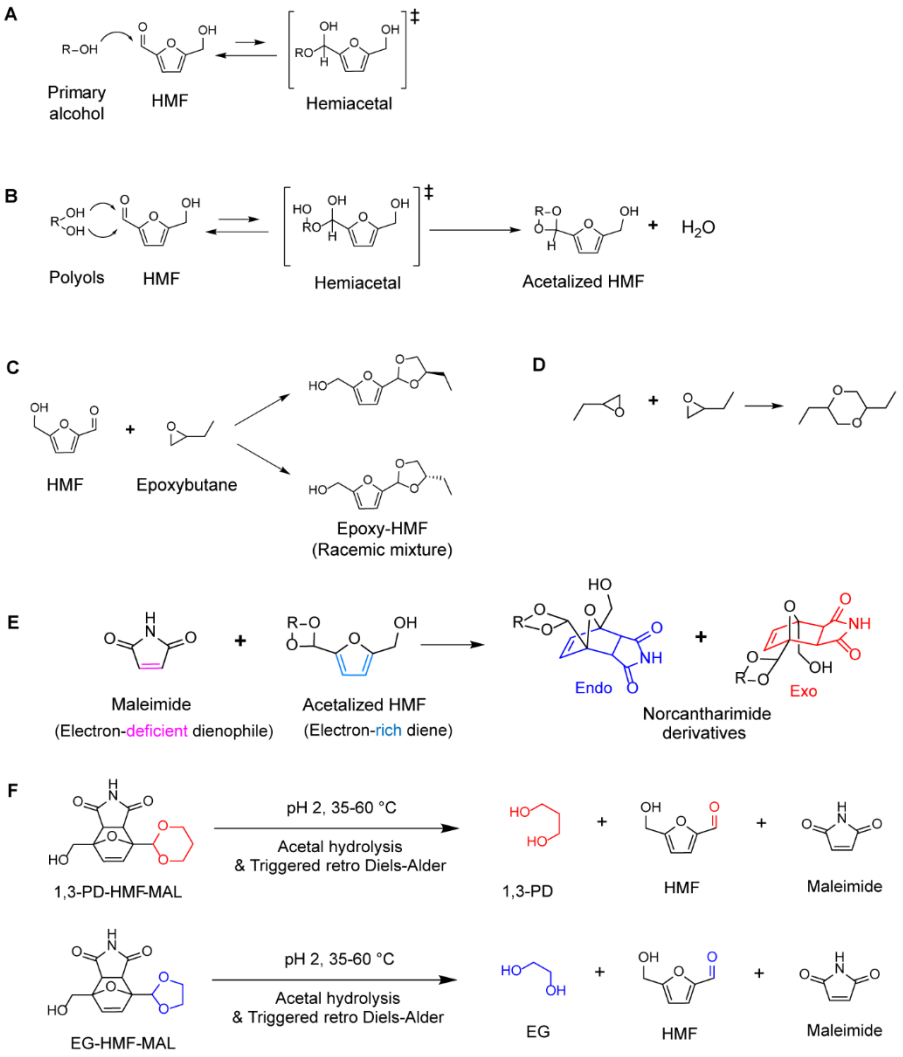

Figure 1. Reaction pathways for acid-catalyzed HMF acetalization with (A) primary alcohols, (B) polyols, (C) epoxybutane, and (D) epoxybutane dimerization; (E) Diels-Alder reaction of

maleimide and acetalized HMF; (F) Chemical release by acetal hydrolysis and triggered retro Diels-Alder reaction.

In subsequent work, we explored the synthesis and properties of functional polyurethanes and polyesters with tunable properties from biomass-derived (HMF)-Acetone-HMF (HAH) monomers. HAH can be selectively hydrogenated over Cu and Ru catalysts to produce partially-hydrogenated HAH (PHAH) and fully-hydrogenated HAH (FHAH). The HAH units in these polymers improve the thermal stability and stiffness of the polymers compared to polyurethanes produced with ethylene glycol. Polyurethanes produced from PHAH provide diene binding sites for electron deficient C=C double bonds, such as in maleimide compounds, that can participate in Diels-Alder reactions. Such sites can function to create crosslinking by Diels-Alder coupling with bismaleimides and can be used to impart functionality to PHAH (giving rise to anti-microbial activity or controlled drug delivery). The symmetric triol structure of FHAH leads to energy-dissipating rubbers with branched structures. Accordingly, the properties of these biomass-derived polymers can be tuned by controlling the blending ratio of HAH-derived monomers or the degree of Diels-Alder reaction.

HAH contains functional groups, including hydroxyl, furan, enone, and ketone functionalities, that can be exploited to further tune the polymer properties. The π-electron conjugation between the enone and furan groups in HAH monomer stabilizes the furan group to prevent the uncontrolled degradation of furans during reactions, such as etherification. Therefore, HAH is a renewable monomer that can be used to synthesize polymers, having high molecular weight (274 g mol^{-1}), symmetric functionalities, an inexpensive production price, and being derived from renewable resources without competition with food resources. We demonstrated the synthesis of functional polyurethanes and a renewable polyester (Figure 2) from HAH-derived monomers, and 4,4'-methylenebis(phenyl isocyanate) (MDI). These biomass-derived polymers have additional chemical functionality that can be used to give the polymer additional properties.

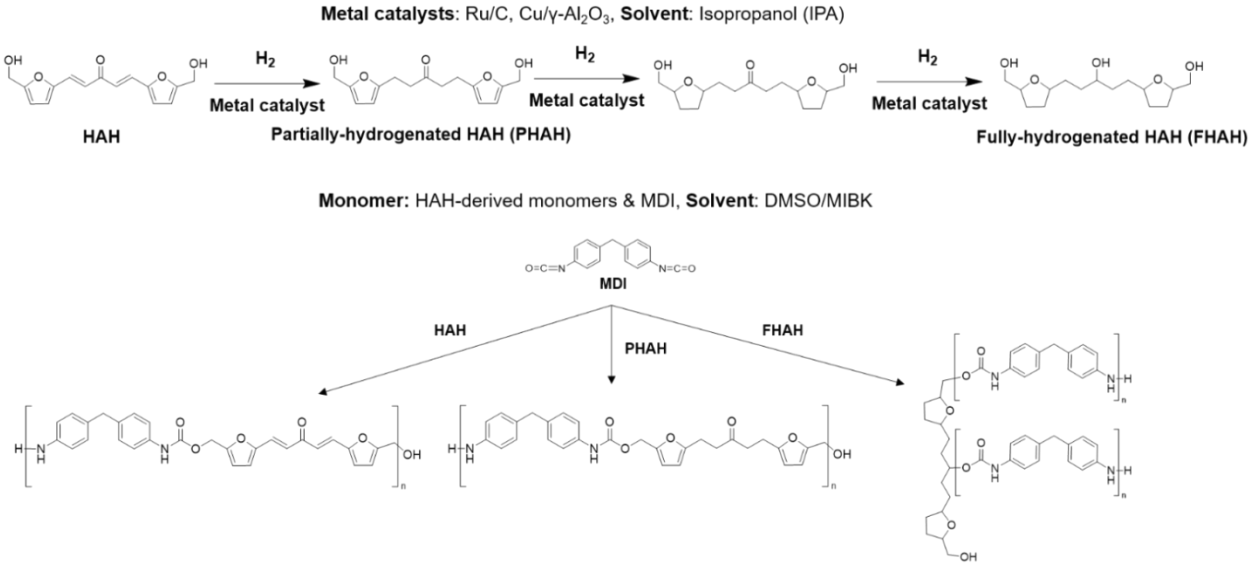

Figure 2. Metal catalyzed hydrogenation of HAH to produce partially-hydrogenated HAH (PHAH) and fully-hydrogenated HAH (FHAH) for production of HAH-derived monomers and

the polymerization of HAH-derived monomers with MDI for production of HAH-derived polymers.

As outlined in the above results, we showed that it is essential to be able to selective hydrogenate C=C double bonds in HAH to be able to achieve effective Diels Alder reactions of the furan ring. Therefore, we studied the hydrogenation at temperatures from 313 – 393 K of HAH over Pd, Ru, and Cu based catalysts. HAH was selectively hydrogenated to produce partially-hydrogenated HAH monomers (PHAH) over Cu and Ru catalysts and to fully-hydrogenated HAH monomers (FHAH) over the Ru catalyst. Pd based catalysts yielded a mixture of partially and fully hydrogenated monomers. Reaction kinetics models were employed to quantify the kinetic behavior for hydrogenation over Ru, Cu, and Pd catalysts. A 5-step pathway exhibited over Pd and Ru catalysts consists of both series and parallel reaction steps, where HAH is both converted to fully hydrogenated products sequentially via series reactions of partially hydrogenated intermediates, as well as converted directly in parallel reactions to form the fully hydrogenated products. In contrast, a 3-step pathway over the Cu catalyst consists only of the consecutive reaction steps, where the final product was formed via series reactions of intermediate products. Additionally, reaction over the Cu catalyst did not hydrogenate the furan rings of the HAH molecule and yielded a different final product than those hydrogenation over Pd and Ru catalysts. Batch conditions were determined for each hydrogenated product that give the highest yields in both batch and plug flow reactors.

Figure 3 depicts pathways for hydrogenation of HAH over Pd catalysts to various partially and fully hydrogenated products. As the C=C bonds in the enone bridge and furan rings are hydrogenated, more rotation and flexibility are imparted to the molecule. The degree of hydrogenation of HAH altered the physical and thermal properties of polymer products synthesized from these hydrogenated monomers.

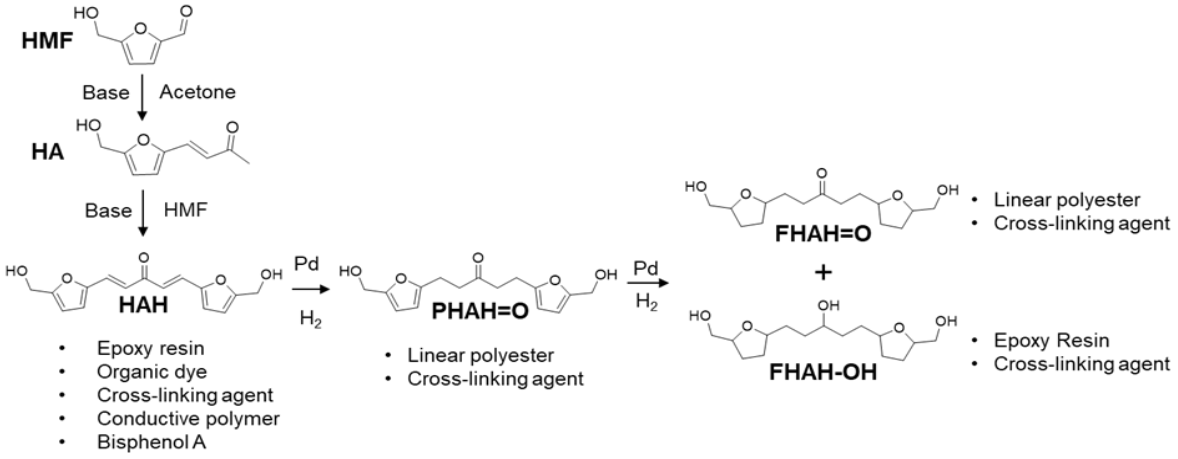

Figure 3. Formation of HAH from Diels-Alder reaction of HMF and acetone, followed by Pd-catalyzed hydrogenation to various hydrogenation products.

Using the results from our reaction kinetics studies, we investigated the optimized reaction conditions for controlled hydrogenation of HAH by calculating apparent rate constants, activation energies, and orders for the selective hydrogenation of HAH over Pd, Ru, and Cu surfaces. We then used the kinetic model to predict optimized product yields using the kinetic data from Arrhenius plots. Figure 4 depicts the optimized yields of each hydrogenation product

along a universal x-axis, X(Batch / PFR), derived from batch and plug flow reactor (PFR) design equations in Eqn. 1 and Eqn. 2:

Eqn. 1
$$\frac{dC_i}{dt} = \left[\frac{m_{Batch}}{V_R}\right] \sum_j k_j f_j(C_k)$$

Eqn. 2
$$\frac{dC_i}{d(z)} = \left[\frac{m_{PFR}}{\upsilon_{liq}}\right] \sum_j k_j f_j(C_k)$$

where t represents the time in the batch reactor (min), m_{Batch} and m_{PFR} represent the total mass of catalyst used in the batch and PFR reaction, respectively (g), and V_R and υ_{liq} are the volume of the liquid volume of the batch reactor (L) and the liquid flow rate in the PFR (L min^{-1}). Finally, z is the mass of the catalyst bed reacted normalized by the total mass of the bed. As such, z is equal to 1 at the outlet of the PFR reactor bed. By integrating and equating Eqn. 1 and Eqn. 2, we can derive a simple equation for X(Batch/PFR), representing either a function of time in a batch reactor or the total weight ratio of a plug flow reactor:

Eqn. 3
$$\frac{dC_i}{dXBatch/PFR} = \sum_j k_j f_j(C_k)$$

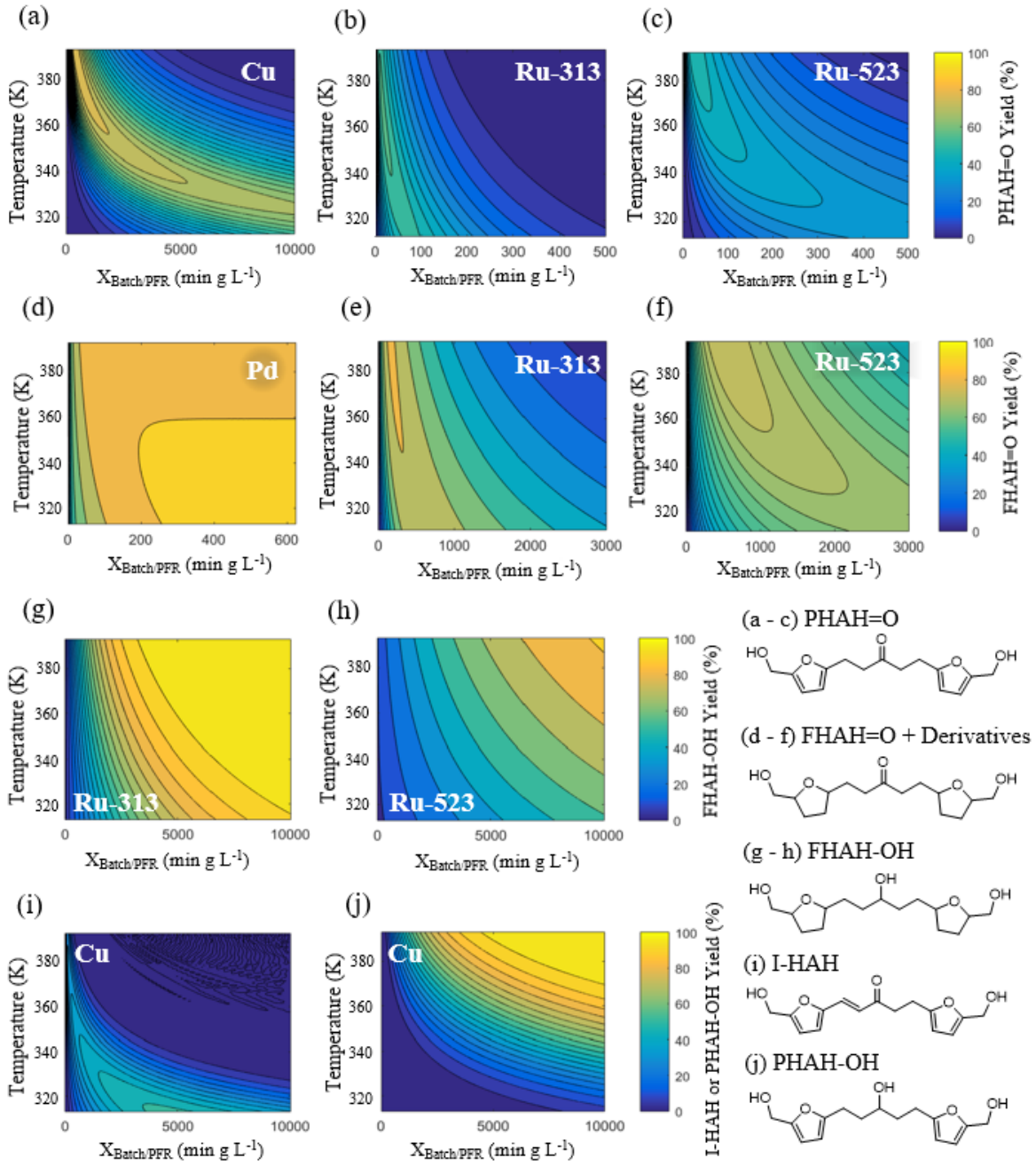

$$X_{Batch\ /\ PFR} = t\frac{m_{Batch}}{V_R} = z\frac{m_{PFR}}{\upsilon_{liq}}$$

Figure 4. Universal yield plots for optimized production of (a – c) PHAH=O, (d – f) FHAH=O and derivatives, (g – h) FHAH-OH, (i) I-HAH, and (j) PHAH-OH in batch and plug flow reactors from 313 – 393 K over Pd/Al_2O_3, Ru/C (Ru-313 or Ru-523), and Cu/Al_2O_3 catalysts.

The plots in Figure 4 size the reactor or determines the required flow rate and catalyst weight for a batch or PFR system at the optimal conditions to produce hydrogenated HAH monomers of interest over the optimal catalyst, per the reaction kinetics parameters determined from this study. From the optimal yield results, PHAH=O was found to be produced with moderate-to-high selectivity over Cu and both Ru catalysts. The maximum PHAH=O yield is

visible in Figure 4a, which shows a yield of 78.7% PHAH=O at X_(Batch/PFR)= 415 min g L^{-1}) over Cu/Al_2O_3 at 393 K. Ru-313/C yielded higher predicted maximum PHAH=O (56%) than the optimal PHAH=O yields predicted over Ru-523/C (50 %) in the examined temperature range. FHAH=O and corresponding derivatives were predicted to have a maximum combined yield over Pd (92.2% at 313 K). The yield was found to increase with decreasing temperature. This prediction was close to the experimentally observed yield over Pd of 85% at 313 K. In the universal yield plot in Figure 4(d), this maximum yield occurs at X(Batch/PFR)= 625 min g L^{-1}. FHAH=O and its derivatives were also yielded over both Ru catalysts. Yields are predicted to increase with temperature over Ru-523/C and Ru-313/C, and reach maxima of 75.1% and 81.6%, respectively, at 393 K. However, Ru-313/C was more active, as seen when comparing the time scales of Figure 4(e) and (f), yielding maximum FHAH=O at X(Batch/PFR)= 155 min g L^{-1}. Figure 4(g) and (h) shows that FHAH-OH was predicted to achieve ~100 % yield over both Ru catalyst as the final product in the sequential hydrogenation reaction scheme. However, faster production with lower catalyst weights was predicted over the untreated Ru/C compared to Ru/C after reduction. FHAH-OH production over Ru-313/C was optimized at 99.9% yield at X(Batch/PFR)= 7250 min g L^{-1}. While full conversion of HAH to FHAH-OH is possible at low temperatures, higher temperatures afforded shorter reaction times, and suffered little penalty of degradation reactions, as few unknown compounds were observed over Ru catalysts throughout the investigated temperature range (313 – 393 K). Two additional compounds were identified in this study over the Cu/Al2O3 catalyst. I-HAH was produced in lower but moderately selective yields (51%). Low temperatures were found to favor higher I-HAH yields. Cu/Al_2O_3 was also the only catalyst that yielded PHAH-OH. PHAH-OH yields were found to increase with increasing temperature. PHAH-OH yields were optimized at X(Batch/PFR)= 9900 min g L^{-1}, yielding 99.9% conversion to the final hydrogenation product along the reaction scheme over Cu.

In summary, we demonstrated that the reaction kinetics of HAH hydrogenation can be modelled by combined parallel and sequential lumped pathways with first order dependences of HAH and intermediate concentrations over Pd, Ru, and Cu catalysts. We also predict optimal conditions and product yields from the lumped model and suggest conditions for further investigation of selective hydrogenation for various HAH derived products. Pd demonstrates a 4-step hydrogenation scheme that is dominated by parallel steps and yields a mixture of partially and fully hydrogenated products (FHAH=O and FHAH-OH). Ru catalysts show a 5-step hydrogenation scheme that terminates in FHAH-OH, with the Ru catalyst undergoing no pre-reduction exhibiting a larger contribution of consecutive steps dominating the hydrogenation scheme. Hydrogenation over Cu exhibits a 3-step reaction scheme and yields significant concentrations of an intermediate previously seen in small quantities over Pd and Ru catalysts. HAH hydrogenation over Cu also terminates in a different final hydrogenation product, PHAH-OH, a triol where all furan rings remained intact. Hydrogenation of furan rings was not observed over Cu. The maximum experimental yields obtained for hydrogenation intermediate products PHAH=O and FHAH=O (and derivatives) were 85% over Cu and 85% over Pd, and full conversion to FHAH-OH and PHAH-OH was possible over both Ru catalysts and the Cu catalyst, respectively.

In subsequent work, we employed reaction schemes to optimize the yields of products from selective hydrogenations of HAH in isopropanol solvent and in the presence of liquid water. Reaction schemes consisting of 7, 9, and 11 steps were examined to describe the rates of formation

of the observed products and reaction intermediates for hydrogenation of HAH over Ru and Pd catalysts, and a 3-step scheme was studied over Cu catalysts. Rate constants and activation energies were calculated using these reaction schemes, and we then apply these reaction schemes to explore the effects of water addition on the hydrogenation pathways. The effects of water addition to isopropanol (IPA) solvents on the hydrogenation of HAH were markedly different over Pd, Ru, and Cu catalysts. Over the Pd catalyst, the addition of water to IPA increased hydrogenation rates and promoted hydrogenation of furan rings. The addition of water to IPA yielded significant carbon losses over the Ru catalyst, and slowed hydrogenation steps over Cu, while significantly inhibiting hydrogenation of the ketone group. This behavior opened routes toward increased production rates of PHAH=O (a partially hydrogenated form of HAH containing a C=O bond), a product in which the diene groups of the furan rings were not hydrogenated. Addition of water also allowed increased feed concentrations of HAH that were previously not possible in pure IPA solvents. This study also identified two additional reaction intermediates into the pathway that were previously assigned as derivatives of FHAH=O, the form of HAH in which all double bonds except the ketone C=O bond have been hydrogenated.

We examined reaction schemes for the hydrogenation of a biomass-derived platform chemical (HAH) from HMF. Two partially hydrogenated intermediates, I-PHAH=O and I-PHAH-OH, were assigned and incorporated into the HAH hydrogenation schemes over Pd and Ru catalysts. Reaction schemes consisting of 7, 9 and 11 steps were examined to determine the optimal number of direct reaction pathways within the hydrogenation scheme. The 11-step mechanism was found to best describe the behavior over Pd and Ru catalysts without overfitting. Reaction rate constants and apparent activation energies were calculated and examined to elucidate the reaction behavior over Pd and Ru catalysts. The reaction kinetics parameters showed that the hydrogenation of a single furan ring (i.e. in I-PHAH=O and I-PHAH-OH) significantly inhibited further hydrogenation over Pd/Al2O3 catalysts in IPA by at least 1 order of magnitude, while the direct hydrogenation of both furan rings completely prevented further hydrogenation. This behavior suggests a repulsion of tetrahydrofuran rings from the Pd surface, limiting further adsorption and reaction of the entire molecule. Similar behavior for hydrogenated furan rings was not detected over Ru surfaces.

We applied the 11-step reaction scheme to understand the effects of water addition in an isopropanol-water cosolvents system over Pd and Ru catalysts, and further examined the effects of water addition on a Cu catalyst using a 3-step sequential hydrogenation scheme. IPA-water cosolvents had markedly different effects over each metal surface examined. Over Pd/Al_2O_3, the addition of water to the solvent system promoted hydrogenation of the furan rings. IPA-water cosolvents also facilitated complete conversion of the partially hydrogenated intermediate compounds (i.e. I-PHAH=O and I-PHAH-OH) to the fully hydrogenated triol, FHAH-OH, rather than to the ketone product, FHAH=O. Over Ru catalysts, water addition was found to severely decrease carbon balances, even at the lowest temperature (313 K). Water addition over the Cu catalyst decreased reaction rate constants for all steps, but strongly inhibited hydrogenation of the ketone group. The overall production rate of PHAH=O can be increased by leveraging higher HAH solubility afforded in IPA-water co-solvents and increasing HAH feed concentrations. PHAH=O was selectively produced with high carbon balances (over 95%) at higher reactant concentrations, yielding 84% PHAH=O at 0.14 M of HAH and 78% PHAH=O at 0.28 M HAH. This work adds to knowledge of liquid phase hydrogenation of dimer molecules and adds understanding of how

various functional groups interact with Pd, Ru, and Cu catalysts in the presence of water, and can open further avenues of additional solvent effects on HAH hydrogenation.

In our most recent work at the end of the grant period, we have employed HAH-derived molecules to append N-substituted maleimides with amino acid (glutamic acid) substitution by Diels-Alder reaction to mimic the chemical functional groups that comprise the active site channels in enzyme catalysts. The difunctionality of the biomass-derived difuran allows production of Diels-Alder adducts by appending two amino acid moieties to form a difunctional organocatalyst. The catalytic activity of the organocatalyst can be improved by immobilizing the organocatalyst on solid supporting materials. Accordingly, the structures of these immobilized organocatalysts can be engineered to mimic enzymatic active sites and to control the interaction between reactants, products, and transition states of catalytic reactions. We carried out lactose hydrolysis to provide an example of industrial application of this approach to design and fabricate new supported organocatalysts as artificial enzymes.

At the current time, we are collaborating with the research group of Professor Mavrikakis to use electronic structure calculations employing density functional theory to understand the detailed mechanistic aspect of the selective hydrogenation of HAH over copper surfaces.

Publications resulting from this work regarding the

synthesis and catalytic hydrogenation of HAH

(1) Hochan Chang, George W. Huber, and James A. Dumesic, Chemical-Switching Strategy for Synthesis and Controlled Release of Norcantharimides from a Biomass-Derived Chemical, *ChemSusChem* **13**, 5213 (2020).

(2) Hochan Chang, Elise B. Gilcher, George W. Huber, and James A. Dumesic, Synthesis of performance-advantaged polyurethanes and polyesters from biomass-derived monomers by aldol-condensation of 5-hydroxymethyl furfural and hydrogenation, *Green Chemistry* **23**, 4355 (2021).

(3) Hochan Chang, Elise B. Gilcher, George W. Huber, and James A. Dumesic, Design of closed-loop recycling production of a Diels-Alder polymer from a biomass-derived difuran as a functional additive for polyurethanes, *Green Chemistry* **23**, 9479 (2021).

(4) Elise B. Gilcher, Hochan Chang, George W. Huber, and James A. Dumesic, Controlled hydrogenation of a biomass-derived platform chemical formed by aldol-condensation of 5-hydroxymethyl furfural (HMF) and acetone over Ru, Pd, and Cu catalysts, *Green Chemistry* **24**, 2146 (2022).

(5) Elise B. Gilcher, Hochan Chang, George W. Huber, and James A. Dumesic, Effects of Water Addition to Isopropanol for Hydrogenation of Compounds Derived from 5-hydroxymethyl furfural over Pd, Ru, and Cu Catalysts, *ACS Catalysis* **12**, 10186 (2022).